

Uplink Sum-Rate Maximization for Pinching Antenna-Assisted Multiuser MISO Communications

Jiarui Zhang, Hao Xu, Chongjun Ouyang, Qiuyun Zou, Hongwen Yang

Abstract—This article investigates the application of pinching-antenna systems (PASS) in multiuser multiple-input single-output (MISO) communications. Two sum-rate maximization problems are formulated under minimum mean square error (MMSE) decoding, with and without successive interference cancellation (SIC). To address the joint optimization of pinching antenna locations and user transmit powers, a fractional programming-based approach is proposed. Numerical results validate the effectiveness of the proposed method and show that PASS can significantly enhance uplink sum-rate performance compared to conventional fixed-antenna designs.

Index Terms—Multiuser communications, pinching antennas, sum-rate maximization, uplink transmission.

I. INTRODUCTION

THE advent of 6G communication systems calls for the application of flexible-antenna technologies, such as fluid antennas [1] and movable antennas [2]. These technologies have some limitations that they cannot have a large-scale antenna reconfiguration and lack the flexibility to add or move antennas.

To solve these problems, pinching antennas (PAs) has introduced by NTT DOCOMO in 2021 [3], [4], which leverage dielectric waveguides for flexible transmission as shown in Fig. 1. Electromagnetic waves are emitted by pinching small dielectric particles at specific points along the waveguide [5]. Similar to adding or removing a clothespin from a clothesline, these dielectrics are typically attached to the tips of plastic clips and can be dynamically added or removed from the waveguide for precisely serving wireless communications [6].

Recent studies have highlighted several advantages of PAs [7]. Unlike the conventional flexible-antenna systems, PAs mitigate large-scale path loss by adjusting PA placement across waveguide. This procedure referred to as “pinching beamforming”, which enhance network coverage and “last-meter” connectivity [6]. Besides, PAs offer scalability in adding or removing antennas and reconfigure the channel environment at low cost and low complexity. These take the benefits of outperforming traditional fixed-antenna designs in large coverage areas. In essence, PASS can be viewed as a specific implementation of fluid-antenna or movable-antenna concepts, which offers a more flexible and scalable solution than traditional architectures. In recognition of DOCOMO’s contribution, we refer to this technology as PASS throughout this paper.

These benefits have spurred significant research into pinching-antenna systems (PASS). Up to now, most studies considered downlink transmission. The work in [8] was the first theoretical study on the PASS and focused on the practical

designs. This research considered about a multiuser multiple-input single-output (MISO) PASS with one waveguide and multiple PAs, and the result showed that PASS can motivate the application of nonorthogonal multiple access. Meanwhile, the authors in [9] optimized PA positioning for a downlink system, where multiple pinching antennas are deployed on a waveguide to serve a single-antenna user. The activation of PAs along one waveguide is further considered in [10] to serve multiple users. To establish an accurate signal model, the authors in [11] first indicated the electromagnetic field behavior and proposed a physics-based hardware model for PASS. Besides, some learning-based methods were proposed in [12], [13] to realize the efficient beamforming in PASS, which can be applied to the situation of one waveguide with multiple PAs.

The above studies validated the effectiveness of PASS in wireless communication. However, all these studies considered the downlink scenarios. For uplink transmission, the authors in [14] and [15] analysed the performance of uplink system with multiple users and orthogonal multiple access (OMA), respectively, which were limited to scenarios where all PAs are positioned within a single waveguide. It is noted that there is no research considering deploying multi-waveguides in uplink multiuser communications, which results in a joint optimization problem of users’ power and pinching beamforming. Therefore, despite its importance, how to improve the uplink sum-rate for pinching antennas assisted multiuser systems with multiple waveguides still remains an open problem.

To fill the research gap, this paper investigates uplink transmission for multiuser multiple input single output (MISO) systems with PAs employed in multi-waveguides. Our contributions are summarized as follows: i) We propose the frame of uplink PASS with multiple waveguides. ii) We formulate a optimization problem respecting PAs’ positions and users’ power under two classic combining rules—minimum mean square error (MMSE) with successive interference cancellation (SIC) and without SIC [16]. iii) We propose an efficient fractional programming (FP)-based algorithm [17] in a structure of block coordinate descent (BCD) to jointly optimize PAs’ positions and user power allocation. iv) We present numerical results to demonstrate that the proposed method outperforms conventional methods in sum-rate performance by increasing system flexibility.

II. SYSTEM MODEL AND PROBLEM FORMULATION

Consider a PASS-assisted uplink MISO communication system consisting of N dielectric waveguides and M single-antenna users, as illustrated in Fig. 1.

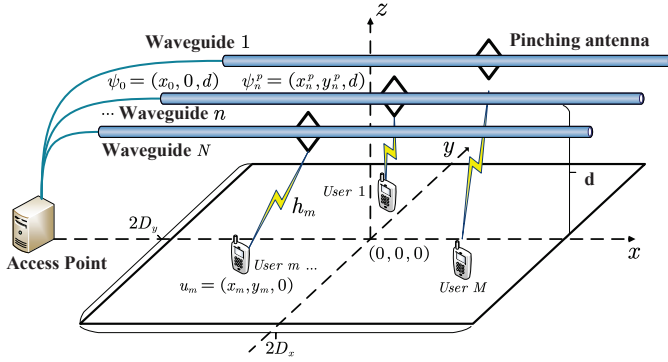


Fig. 1: Illustration of a PASS-assisted multiuser MISO uplink channel.

A. Pinching-Antenna System

We assume that each PA is activated on different waveguides, jointly serving the users. Each pinching element can freely move across different waveguides and transmit signal to the access point. Waveguides are extended over the x -axis at the altitude d in an array formed on the y -axis with each two waveguides being distanced $\frac{D_y}{N}$. The location of pinching element n on the waveguide $n \in [N]$ in the Cartesian coordinate is given by $\psi_n^p = [x_n^p, y_n^p, d]$, where $x_n^p \in [-D_x, D_x]$ and $y_n^p = -D_y + \frac{nD_y}{N}$.

The users are distributed within a known two-dimensional area, e.g., a rectangular region. The m th user is located at $\mathbf{u}_m = [x_m, y_m, 0]^T$ for $\forall m \in \mathcal{M} = \{1, \dots, M\}$ and transmits its signal to the access point located at $\psi_0 = [x_0, 0, d]$ with $x_0 < 0$. Specifically, x_m and y_m are subject to the constraints of $x_m \in [-D_x, D_x]$, $y_m \in [-D_y, D_y]$, assuming that the users are located in the xy -plane.

The spatial channel between the m th user and the PASS can be expressed as follows [8]:

$$\mathbf{h}_m = [h_{m,1}, \dots, h_{m,N}]^T = \left[\frac{\eta^{\frac{1}{2}} e^{-j\frac{2\pi}{\lambda} \|\mathbf{u}_m - \psi_n^p\|}}{\|\mathbf{u}_m - \psi_n^p\|} \right]_{n=1}^N, \quad (1)$$

where $\eta = \frac{c^2}{16\pi^2 f_c^2}$, c denotes the speed of light, f_c is the center frequency, and λ is the wavelength in the free space equal to $\frac{c}{f_c}$. Considering about the phase shift of received signals by the N PAs, we define $\phi = [e^{-j\phi_1}, \dots, e^{-j\phi_N}]^T \in \mathbb{C}^{N \times 1}$, where $\phi_n = \frac{2\pi}{\lambda_g} (x_n^p - x_0)$, and $\lambda_g = \frac{\lambda}{n_{\text{eff}}}$, with n_{eff} representing the effective refractive index of the dielectric waveguide [18].

Taken together, the effective channel between the m th user and the PASS can be expressed as $\mathbf{g}_m = \phi \circ \mathbf{h}_m$, where \circ denotes the Hadamard product. The received signal at the PASS is given by

$$\mathbf{y} = \sum_{m=1}^M \sqrt{p_m} \mathbf{g}_m s_m + \mathbf{n}, \quad (2)$$

where $s_m \sim \mathcal{CN}(0, 1)$ denotes the symbol transmitted by the m th user with $\mathbb{E}\{s_i s_j^*\} = 0, \forall i \neq j$, $\mathbf{n} \sim \mathcal{CN}(0, \sigma^2 \mathbf{I}_N)$ is additive white Gaussian noise with power σ^2 , and p_m presents the transmit power of the m th user, subject to $p_m \leq p_{\max}$, where p_{\max} is the maximum power. After receiving the signal, BS employ two different combining rules, MMSE-SIC and

MMSE-nSIC combiner [16]. The sum-rate with these are given by (3) and (4), as shown at the top of next page. Note that the decoding order of MMSE-SIC method has no influence of the sum-rate. Thus, to simplify the analysis, we assume that the decoding order of MMSE-SIC method is from the 1st user to the M th user.

B. Problem Formulation

We aim to maximize the sum-rate of the considered uplink PASS by jointly optimizing the power of users and positions of PAs. The optimization problem can be formulated as follows:

$$\mathcal{P}_X : \max_{\mathbf{P}, \Psi^p} \mathcal{R}_X \quad (5a)$$

$$\text{s.t. } 0 \leq p_m \leq P_{\max}, \quad \forall m \in \mathcal{M}, \quad (5b)$$

$$x_n^p \in [-D, D] \quad \forall n \in \mathcal{N}, \quad (5c)$$

where $\mathbf{p} = [p_m]_{m=1}^M$, $\Psi^p = [\psi_n^p]_{n=1}^N$, $X \in \{\text{sic}, \text{nsic}\}$.

III. PROPOSED METHOD

A. MMSE-SIC case

Solving the optimization problem \mathcal{P}_{sic} is highly challenging due to several points. First, the objective function of \mathcal{P}_{sic} is non-convex with respect to the variables $\{\mathbf{P}, \Psi^p\}$. In addition, minor changes in antenna positions can result in significant phase variations at high-frequency bands, which indicates that positioning needs an optimization algorithm with higher accuracy. To develop a computationally efficient algorithm, we exploit the fractional programming framework [17] and introduce two sets of auxiliary variables to transform \mathcal{P}_{sic} into a new problem with a more manageable objective function, while maintaining the equivalence of the original problem. The following two lemmas lay the groundwork for this transformation.

Lemma 1. Problem \mathcal{P}_{sic} is equivalent to

$$\mathcal{P}_1 : \max_{\mathbf{P}, \Psi^p} \mathcal{F}_1(\boldsymbol{\alpha}, \mathbf{P}, \Psi^p) \triangleq \sum_{m=1}^M \log(1 + \alpha_m) - \sum_{m=1}^M \alpha_m + \sum_{m=1}^M (1 + \alpha_m) \mathcal{A}_m \quad (6a)$$

$$\text{s.t. (5b), (5c), } \alpha_m > 0, m = 1, \dots, M, \quad (6b)$$

$$\text{where } \mathcal{A}_m \triangleq p_m \mathbf{g}_m^H \left(\sum_{i=m}^M \mathbf{g}_i \mathbf{g}_i^H p_i + \sigma^2 \mathbf{I}_N \right)^{-1} \mathbf{g}_m, \\ \boldsymbol{\alpha} = [\alpha_1, \dots, \alpha_M]^T, \text{ where the optimal } \alpha_m \text{ is given by} \\ \alpha_m^\dagger \triangleq p_m \mathbf{g}_m^H \left(\sum_{i=m+1}^M \mathbf{g}_i \mathbf{g}_i^H p_i + \sigma^2 \mathbf{I}_N \right)^{-1} \mathbf{g}_m. \quad (7)$$

Proof: Let $\{\boldsymbol{\alpha}^\dagger, \mathbf{P}^\dagger, \Psi^{p\dagger}\}$ denote the optimal solution of \mathcal{P}_1 . Then, $\max_{\boldsymbol{\alpha}, \mathbf{P}, \Psi^p} \mathcal{F}_1 = \max_{\mathbf{P}, \Psi^p} \mathcal{F}_1(\boldsymbol{\alpha}^\dagger, \mathbf{P}, \Psi^p)$ and $\{\mathbf{P}^\dagger, \Psi^{p\dagger}\} = \text{argmax}_{\mathbf{P}, \Psi^p} \mathcal{F}_1(\boldsymbol{\alpha}^\dagger, \mathbf{P}, \Psi^p)$. Given the analysis of \mathcal{F}_1 across the entire complex plane and its concavity with respect to $\boldsymbol{\alpha}$ for a fixed set $\{\mathbf{P}, \Psi^p\}$, we derive its complex gradient and resolve the condition $\frac{\partial \mathcal{F}_1}{\partial \alpha_m} = 0$ for every index m . Thus, the optimized $\boldsymbol{\alpha}$ is obtained as $\alpha_m^\dagger = \frac{\mathcal{A}_m}{1 - \mathcal{A}_m}$, which can be derived as shown in (7) using the Woodbury formula. Inserting α_m^\dagger back to \mathcal{F}_1 yields $\mathcal{F}_1(\boldsymbol{\alpha}^\dagger, \mathbf{P}, \Psi^p) =$

$$\mathcal{R}_{\text{sic}} = \sum_{m=1}^M \log \left(1 + p_m \mathbf{g}_m^H \left(\sum_{i=m+1}^M \mathbf{g}_i \mathbf{g}_i^H p_i + \sigma^2 \mathbf{I}_L \right)^{-1} \mathbf{g}_m \right), \quad (3)$$

$$\mathcal{R}_{\text{nsic}} = \sum_{m=1}^M \log \left(1 + p_m \mathbf{g}_m^H \left(\sum_{i \neq m}^M \mathbf{g}_i \mathbf{g}_i^H p_i + \sigma^2 \mathbf{I}_L \right)^{-1} \mathbf{g}_m \right), \quad (4)$$

\mathcal{R}_{sic} . Hence, we can get $\max_{\alpha^\dagger, \mathbf{P}, \Psi^p} \mathcal{F}_1 = \max_{\mathbf{P}, \Psi^p} \mathcal{R}_{\text{sic}}$ and $\text{argmax}_{\mathbf{P}, \Psi^p} \mathcal{F}_1(\alpha^\dagger, \mathbf{P}, \Psi^p) = \text{argmax}_{\mathbf{P}, \Psi^p} \mathcal{R}_{\text{sic}}$, which suggests that \mathcal{P}_{sic} and \mathcal{P}_1 have the same optimal objective value as well as the same optimal solution to $\{\mathbf{P}, \Psi^p\}$. ■

With the help of Lemma 1, \mathcal{P}_{sic} becomes more manageable. However, it still involves a matrix inversion term, making it a non-convex problem. To further address this, we employ the FP-based approach and introduce auxiliary variables $\beta = \{\beta_1, \dots, \beta_M\}$ to simplify $\mathcal{F}_1(\alpha, \mathbf{P}, \Psi^p)$. The lemma 2 is shown as follows.

Lemma 2. Problem \mathcal{P}_1 is equivalent to the following:

$$\mathcal{P}_2 : \max_{\mathbf{P}, \Psi^p} \mathcal{F}_2(\alpha, \beta, \mathbf{P}, \Psi^p) \triangleq \sum_{m=1}^M \log(1 + \alpha_m) - \sum_{m=1}^M \alpha_m + \sum_{m=1}^M \left[2\sqrt{1 + \alpha_m} \Re(\beta_m^H \mathbf{g}_m \sqrt{p_m}) - \beta_m^H \left(\sum_{i=m}^M \mathbf{g}_i \mathbf{g}_i^H p_i + \sigma^2 \mathbf{I}_N \right) \beta_m \right] \quad (8a)$$

$$\text{s.t. (6b), } \beta_m \in \mathbb{C}^{N \times 1}, m \in \mathcal{M}, \quad (8b)$$

where each β_m has the following optimal solution

$$\beta_m^\dagger = \sqrt{1 + \alpha_m} \left(\sum_{i=m}^M \mathbf{g}_i \mathbf{g}_i^H p_i + \sigma^2 \mathbf{I}_N \right)^{-1} \sqrt{p_m} \mathbf{g}_m. \quad (9)$$

Proof: The proof is similar to that of Lemma 1. Note that when $\alpha, \mathbf{P}, \Psi^p$ are fixed, \mathcal{F}_2 is concave with respect to β . Therefore, by taking its complex derivative and solving the condition $\frac{\partial \mathcal{F}_2}{\partial \beta_m} = 0$, the optimal solution for β_m is β_m^\dagger in (9). Following a similar approach as in the proof of Lemma 1, Lemma 2 can be established. ■

Based on Lemmas 1 and 2, it is worth noting that problem \mathcal{P}_2 has a more tractable objective function than \mathcal{P}_{sic} , which is in terms of concerning each variable with others fixed. To solve problem \mathcal{P}_2 , we propose a block coordinate descent algorithm by sequentially updating $\alpha, \beta, \mathbf{P}, \Psi^p$.

1) *Optimize α and β :* We first optimize α with the other variables fixed. Specifically, by checking its first-order optimality condition, the optimal α can be obtained, i.e., α_m^\dagger in (7). Similarly, by fixing other variables and checking their first-order optimality condition, the optimal solution to β is given by β_m^\dagger in (9).

2) *Optimize Ψ^p :* Then we investigate the optimization of the PAs position by fixing other variables. The subproblem for

Ψ^p is formulated as:

$$\mathcal{P}_3 : \max_{\Psi^p} f_1(\Psi^p) \triangleq \sum_{m=1}^M \left[2\sqrt{1 + \alpha_m} \Re(\beta_m^H \mathbf{g}_m \sqrt{p_m}) - \beta_m^H \sum_{i=m}^M \mathbf{g}_i \mathbf{g}_i^H p_i \beta_m \right] \quad (10a)$$

$$\text{s.t. (5c).} \quad (10b)$$

For each PA, the coordinate Ψ_n^p depends on x_n^p , and f_1 is a one-dimensional function for each x_n when other PA positions are fixed. Specifically, (10a) can be reformulated as:

$$f_2(\Psi^p) \triangleq \sum_{m=1}^M \left[2\eta \sqrt{1 + \alpha_m} \sqrt{p_m} \Re \left(\sum_{n=1}^N \overline{\beta_{m,n}} C_{m,n} \right) - \sum_{i=m}^M \sum_{n=1}^N \sum_{n'=1}^N \eta p_i \overline{\beta_{m,n}} \beta_{m,n'} \overline{C_{m,n}} C_{m,n'} \right], \quad (11)$$

where $C_{m,n} = \frac{e^{-j\phi_n} e^{-j\frac{2\pi}{\lambda} \|\mathbf{u}_m - \psi_n^p\|}}{\|\mathbf{u}_m - \psi_n^p\|}$ and $\beta_{m,n}$ denotes the n -th element of β_m . Given the non-convexity of f_2 , we adopt a the gradient decent method with backtracking line search [19] to optimize x_n^p . The gradient values of $f_2(\Psi^p)$ with respect to x_n^p is derived as follows:

$$\nabla_{x_n^p} f_2 = \sum_{m=1}^M \eta \sqrt{1 + \alpha_m} \sqrt{p_m} \overline{\beta_{m,n}} D_m - E_m - F_m, \quad (12)$$

where

$$D_m = C_{m,n} \frac{x_m - x_n^p}{\|\mathbf{u}_m - \psi_n^p\|^2}, \quad (13a)$$

$$E_m = \sum_{i=m}^M \sum_{n \neq n'}^N \eta p_i \overline{\beta_{m,n}} \beta_{m,n'} \overline{C_{m,n'}} C_{m,n} \frac{x_m - x_n^p}{\|\mathbf{u}_m - \psi_n^p\|^2}, \quad (13b)$$

$$F_m = \sum_{i=m}^M 2\eta p_i |\beta_{m,n}|^2 \frac{e^{-\frac{2j\pi}{\lambda} \|\mathbf{u}_m - \psi_n^p\|} (x_n^p - x_m)}{\|\mathbf{u}_m - \psi_n^p\|^4}. \quad (13c)$$

The proposed GD-based method is summarized in Algorithm 1, which is guaranteed to converge to a stationary-point solution [19] and l_{\min} represents the accuracy less than Armijo step.

3) *Optimize \mathbf{P} :* Finally, by fixing the remaining variables, the optimization problem of \mathbf{P} can be formulated as follows:

$$p_m^\dagger = \text{argmin}_{p_m \leq P_{\max}} \left(f_3(\mathbf{P}) \triangleq p_m B_m - 2\Re(a_m) \sqrt{p_m} \right), \quad (14)$$

where $B_m = \sum_{i=1}^m \mathbf{g}_m^H \beta_i \beta_i^H \mathbf{g}_m$, $a_m = \sqrt{1 + \alpha_m} \beta_m^H \mathbf{g}_m$.

Algorithm 1: GD-Based Method for Optimizing Ψ^p

```

1 Initialize  $\Psi^p(t) = [\psi_1^p(t), \dots, \psi_N^p(t)]$  and  $t = 0$ , step
  size  $l_0$ , the minimum step size  $l_{\min}$ ;
2 repeat
3   for  $n = 1 : N$  do
4     Calculate  $\nabla_{x_n^p}^{(t)} F_2$  and set  $l = l_0$ ;
5     repeat
6       Calculate  $\mathbf{x}_n^p(t+1) = \mathbf{x}_n^p(t) + l \nabla_{x_n^p}^{(t)} F_2$ ;
7       Set  $l = l/3$ ;
8     until  $(5c) \ \& \ F_2(\mathbf{x}_n^p(t+1)) > F_2(\mathbf{x}_n^p(t))$  or
       $l < l_{\min}$ ;
9     if  $l < l_{\min}$  then
10       $\mathbf{x}_n^p(t+1) = \mathbf{x}_n^p(t)$ ;
11   Set  $t = t + 1$ ;
12 until convergence;
```

It's worth noting that maximizing f_3 over \mathbf{P} is a standard convex optimization problem. By exploiting the first-order optimality conditions, we can obtain the optimized \mathbf{P} by setting $\frac{\partial f_2}{\partial p_m} = 0, m = 1, \dots, M$. After some basic mathematical manipulations, the optimal solution \mathbf{P}^\dagger is obtained as follows:

$$p_m^\dagger = \min \left\{ P_{\max}, \frac{\Re(a_m)^2}{B_m^2} \right\}. \quad (15)$$

The proposed BCD-based method for solving (8) is summarized in Algorithm 2. We now provide a brief proof for the convergence of our proposed method. For each iteration, we denote a objective value sequence of (3) as $\{\mathcal{R}_{\text{sic}}(\mathbf{P}^{(j)}, \Psi^{p(j)})\}$, and the objective function of (8) as $\mathcal{F}_2(\alpha^{(j)}, \beta^{(j)}, \mathbf{P}^{(j)}, \Psi^{p(j)})$. Then we have

$$\begin{aligned} \mathcal{R}_{\text{sic}}(\mathbf{P}^{(j+1)}, \Psi^{p(j+1)}) &\stackrel{*}{\geq} \mathcal{F}_2(\alpha^{(j+1)}, \beta^{(j+1)}, \mathbf{P}^{(j+1)}, \Psi^{p(j+1)}) \\ &\geq \mathcal{F}_2(\alpha^{(j)}, \beta^{(j)}, \mathbf{P}^{(j)}, \Psi^{p(j)}) \stackrel{*}{=} \mathcal{R}_{\text{sic}}(\mathbf{P}^{(j)}, \Psi^{p(j)}). \end{aligned} \quad (16)$$

where “ $\stackrel{*}{\geq}$ ” holds due to [17, Section III]. Note that the sequence $\{\mathcal{R}_{\text{sic}}(\mathbf{P}^{(j)}, \Psi^{p(j)})\}$ is monotonous for which is upper bounded due to (5b), thus guaranteeing the convergence of Algorithm 2. Further details can be found in [17]. The computational complexity of our proposed algorithm can be described based on the dimensions of the problem.

Let I_{GD} and I_{BCD} represents the number of the iterations of Algorithm 1 and 2. The per-iteration computational complexity is composed of updating variables $\{\alpha, \beta, \mathbf{P}, \Psi^p\}$. With simple proof, the complex of marginal optimizations w.r.t these scale with $\mathcal{O}(MN^3)$, $\mathcal{O}(MN^3)$, $\mathcal{O}(MN)$ and $\mathcal{O}\left(I_{\text{GD}}NM^2 \log_3\left(\frac{1}{l_{\min}}\right)\right)$. Hence, the overall computational complexity of Algorithm 2 is approximated as $\mathcal{O}\left(I_{\text{BCD}}\left(2MN^3 + MN + I_{\text{GD}}NM^2 \log_3\left(\frac{1}{l_{\min}}\right)\right)\right)$.

B. MMSE-NSIC Case

After solving the uplink sum-rate maximization problem with the MMSE-SIC combining method, we now consider the

Algorithm 2: BCD-Based Method For solving \mathcal{P}_X

```

1 Initialize  $\{\alpha^{(0)}, \beta^{(0)}, \mathbf{P}^{(0)}, \Psi^{p(0)}\}$  and  $j = 0$ ;
2 repeat
3   Update  $\{\alpha^{(j)}, \beta^{(j)}, \mathbf{P}^{(j)}, \Psi^{p(j)}\}$  based on the
  methods stated in 1) – 3), with the equations of
  (7),(9),(15);
4   Set  $j = j + 1$ ;
5 until convergence;
```

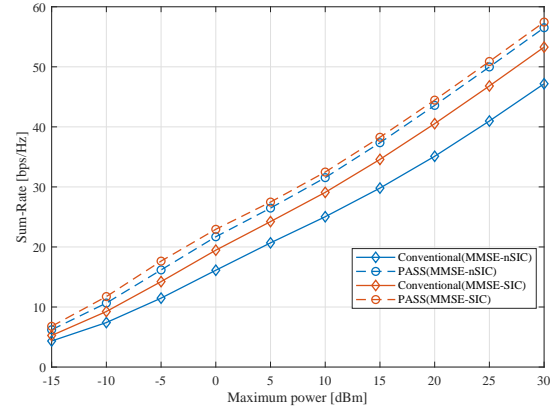


Fig. 2: The sum-rate versus P_{\max} with $N = 4, M = 4$.

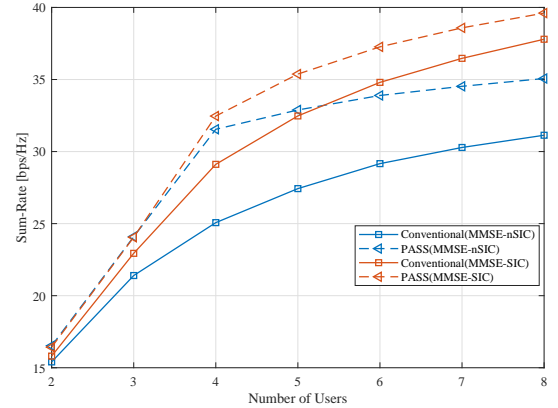


Fig. 3: The sum-rate versus M with $N = 4, P_{\max} = 10$ dBm.

same optimization goal under the MMSE-nSIC, denoted as $\mathcal{P}_{\text{nsic}}$. The objective function for this formulation $\mathcal{R}_{\text{nsic}}$ (as defined in (4)) exhibits structural parallels with the MMSE-SIC version \mathcal{R}_{sic} (defined in (3)). Therefore solving the problem $\mathcal{P}_{\text{nsic}}$ share the same procedures and methodologies of solving \mathcal{P}_{sic} . Detailed derivations are omitted here for brevity.

IV. NUMERICAL RESULTS

This section presents the simulation results of the proposed method with two distinct combining technologies. Specifically, we compare the performance of our proposed method with that of the conventional antenna systems. During the simulation, we set $f_c = 28$ GHz, $D_x = 15$ m, $D_y = 20$ m, $n_{\text{eff}} = 1.4$ [18], $\sigma^2 = -90$ dBm, $d = 5$ m. The users randomly distribute in the xy -plane and PAs are randomly initialized at different

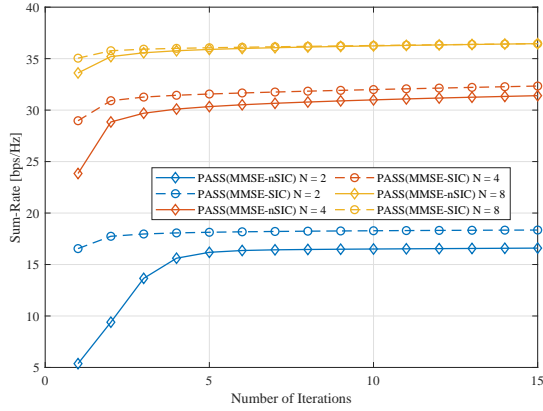


Fig. 4: Convergence with $M = 4$, $P_{\max} = 10$ dBm.

waveguides with in $[-D_x, D_x]$. For the conventional-antenna system, we assume that the BS antennas are located at $\tilde{\psi}_n = [0, \tilde{y}_n, d]$, where $\tilde{y}_n = -D_y + \frac{nD_y}{N}$ for $\forall n \in \mathcal{N} = \{1, \dots, N\}$. This can be viewed as a traditional uniform linear array (ULA) placed at the center of area. All the results are averaged over 10000 independent channel realizations.

Fig. 2 illustrates the impact of users' maximum transmit power on the achievable sum-rate. The results indicate that sum-rate exhibits a monotonically increasing trend with respect to the maximum power allocated to users. Compared to the conventional antenna system with the same combining methods, the proposed PASS has a better performance due to its capability for antenna mobility. The method with SIC is better than nSIC because SIC method considers the proper decoding order to decrease the influence between different users. Notably, within the PASS, SIC method is just a little better than the nSIC method and the performance gap between these two methods ties as the maximum power increases. This demonstrates that through the implementation of the PASS optimization algorithm, the nSIC method with parallel decoding architecture achieves a significantly reduced computational complexity while maintaining the algorithmic performance parity with the SIC approach. This results underscore the critical role played by the PASS optimization algorithm in enabling this performance-complexity trade-off, highlighting its importance in practical communication system design.

Fig. 3 illustrates the observation by showing the sum-rate as a function of the number of users M . It's worth noting that in these two methods, the sum-rate grows rapidly as the user count increases when $M \leq N$, while grows slowly when $M > N$. Besides, the performance gap between these two methods widens as the number of users increases. This highlights the importance of using the SIC method when the user count exceeds the number of antennas.

Finally, the convergence of our proposed BCD-based method is illustrated in fig. 4. As shown, sum-rate converges rapidly for both combiners with different numbers of N . As well as the fig. 2 for the PASS, more antennas reduce the difference of performance between the nSIC method and the SIC method. Thus the nSIC method can apply to the scenario of more antennas with low complexity instead of the SIC

method.

V. CONCLUSION

Our research has investigated the sum-rate maximization for uplink multiuser MISO PASS. The proposed algorithm jointly optimized PA positions and user power allocation with MMSE-SIC and MMSE-nSIC combining rules. This approach not only achieved better sum-rate performance than conventional systems but also highlighted the flexibility and efficiency of PASS. Through simulations, we have validated the effectiveness of our method and demonstrate substantial gains in sum-rate, especially with MMSE-SIC. Our findings suggested that PASS holds great promise for enhancing the spectral efficiency of uplink multi-user communication systems.

REFERENCES

- [1] K.-K. Wong *et al.*, "Fluid antenna systems," *IEEE Tran. Wireless Commun.*, vol. 20, no. 3, pp. 1950–1962, Mar. 2021.
- [2] L. Zhu, W. Ma, and R. Zhang, "Movable antennas for wireless communication: Opportunities and challenges," *IEEE Commun. Mag.*, vol. 62, no. 6, pp. 114–120, Jun. 2024.
- [3] NTT DOCOMO, Inc., "Pinching antenna," https://www.docomo.ne.jp/english/info/mediacenter/event/mwc21/pdf/06MWC2021d_2022.
- [4] A. Fukuda *et al.*, "Pinching antenna: Using a dielectric waveguide as an antenna," *NTT DOCOMO Technical J.*, vol. 23, no. 3, pp. 5–12, Jan. 2022.
- [5] C. Ouyang *et al.*, "Array gain for pinching-antenna systems (PASS)," *arXiv preprint arXiv:2501.05657*, 2025.
- [6] Y. Liu *et al.*, "Pinching-antenna systems (PASS): Architecture designs, opportunities, and outlook," *arXiv preprint arXiv:2501.18409*, 2025.
- [7] Z. Yang *et al.*, "Pinching antennas: Principles, applications and challenges," *arXiv preprint arXiv:2501.10753*, 2025.
- [8] Z. Ding, R. Schober, and H. V. Poor, "Flexible-antenna systems: A pinching-antenna perspective," *IEEE Trans. Commun.*, Early Access, Mar. 2025, doi: 10.1109/TCOMM.2025.3555866.
- [9] Y. Xu, Z. Ding, and G. K. Karagiannidis, "Rate maximization for downlink pinching-antenna systems," *IEEE Wireless Commun. Lett.*, Early Access, Feb. 2025.
- [10] K. Wang, Z. Ding, and R. Schober, "Antenna activation for NOMA assisted pinching-antenna systems," *IEEE Wireless Commun. Lett.*, Early Access, Mar. 2025.
- [11] Z. Wang *et al.*, "Modeling and beamforming optimization for pinching-antenna systems," *arXiv preprint arXiv:2502.05917*, 2025.
- [12] J. Guo, Y. Liu, and A. Nallanathan, "GPASS: Deep learning for beamforming in pinching-antenna systems (PASS)," *arXiv preprint arXiv:2502.01438*, 2025.
- [13] X. Xie, Y. Lu, and Z. Ding, "Graph neural network enabled pinching antennas," *arXiv preprint arXiv:2502.05447*, 2025.
- [14] T. Hou, Y. Liu, and A. Nallanathan, "On the performance of uplink pinching antenna systems (PASS)," *arXiv preprint arXiv:2502.12365*, 2025.
- [15] S. A. Tegos *et al.*, "Minimum data rate maximization for uplink pinching-antenna systems," *IEEE Wireless Commun. Lett.*, Early Access, Mar. 2025.
- [16] D. Tse and P. Viswanath, *Fundamentals of Wireless Communication*. Cambridge U.K.: Cambridge Univ. Press, 2005.
- [17] K. Shen and W. Yu, "Fractional programming for communication systems-Part II: Uplink scheduling via matching," *IEEE Trans. Signal Process.*, vol. 66, no. 10, pp. 2631–2644, May 2018.
- [18] D. M. Pozar, *Microwave Engineering: Theory and Techniques*. Hoboken, NJ, USA: Wiley, 2021.
- [19] S. Boyd and L. Vandenberghe, *Convex Optimization*. Cambridge, U.K.: Cambridge Univ. Press, 2004.